

Imaging cytoskeleton–mitochondrial membrane attachments by embedment-free electron microscopy of saponin-extracted cells

(resinless sections/stereoscopic electron microscopy/scanning electron microscopy)

ANDREW LIN, GABRIELA KROCKMALNIC, AND SHELDON PENMAN*

Department of Biology, Massachusetts Institute of Technology, Cambridge, MA 02139

Contributed by Sheldon Penman, August 14, 1990

ABSTRACT Embedment-free electron microscopy images the cytoskeleton and nuclear matrix, which are very difficult to visualize in conventional electron micrographs. However, to be effective, cell structures must be depleted of soluble proteins, which otherwise shroud cell architecture. Nonionic detergents effect this extraction, releasing soluble proteins but also destroying all membranes. Saponin can permeabilize plasma membranes, releasing soluble proteins while preserving many cytoplasmic membranes. Stereoscopic electron microscopy of resinless sections shows the many connections of the cytoskeleton to mitochondrial membranes.

The complex morphologies and motilities of many cytoplasmic organelles likely reflect tethering to the cytoskeleton. However, little is known of interactions between the cytoskeleton and cytoplasmic membranes since conventional electron microscopy reveals little of their nature. While micrographs of Epon-embedded, ultrathin sections show membranes clearly, the protein networks of the cytoskeleton are invisible. Conversely, embedment-free electron microscopy affords sharp, three-dimensional images of the cytoskeleton of detergent-extracted cells but so far has not been useful for cell membranes. We show here a method for visualizing cytoplasmic membranes and their connections to the cytoskeleton.

The conventional electron microscope thin section was originally developed expressly for examining cell membranes (1). The similar electron-scattering cross-sections of embedding plastic and specimen preclude image formation. Heavy metal atoms, adhered to the section surface, delineate the specimen but only where it emerges from the plastic. Membranes, with osmium as a mordant for binding metal atoms, intersect the section surface, giving clear, meaningful images. Cytoskeleton fibers, for the most part, do not.

In embedment-free electron microscopy, specimens are imaged directly *in vacuo* (2–4). Freed of embedding plastic, biological elements yield high contrast images with no need for staining. However, the embedment-free specimen must be depleted of soluble proteins, which otherwise shroud the cytoskeleton, confounding images to near uselessness. This is most easily done by extraction with a nonionic detergent, such as Triton X-100, in a physiological buffer (5–7). Membranes are solubilized and soluble proteins simply diffuse away. This simple but powerful technique is well suited to imaging three-dimensional structures, which, although invisible in conventional micrographs, afford sharp, well-defined embedment-free images (7–9). The unembedded cytoskeleton and nuclear matrix have proven remarkably rigid and can even be cut into ultrathin sections without excessive deformation (10–14).

We describe an extraction protocol in which saponin, a mild detergent selective for cholesterol (15, 16), permeabilizes the plasma membrane, releasing soluble proteins. Many

membranes survive, and, as an example, we show embedment-free, three-dimensional images of mitochondria and their attachments to the cytoskeleton.

MATERIALS AND METHODS

Cell Culture. HeLa cells (CCL), Caski cervical tumor cells, and rat aortic smooth muscle cells (RASM, a gift from Julia Ingelfinger, Massachusetts General Hospital) were grown in Dulbecco's medium with 10% fetal bovine serum. For whole mounts, HeLa and RASM cells were grown on carbon-coated Formvar films mounted on nickel grids. For resinless section and scanning microscopy, cells were grown on Mylar polyester film (a gift from DuPont).

Cell Extraction and Fixation. Subconfluent cells were pretreated with taxol (5 $\mu\text{g}/\text{ml}$), washed once in phosphate-buffered saline (PBS), and extracted at 4°C with cytoskeleton buffer (CSK; 10 mM Pipes, pH 6.8/100 mM NaCl/300 mM sucrose/3 mM MgCl_2 /2 mM EGTA/4 mM vanadyl riboside complex/1.2 mM phenylmethylsulfonyl fluoride) containing either 0.01% (vol/vol) saponin (Sigma) for 7 min or 0.5% (vol/vol) Triton X-100 for 1 min. Cells were then fixed with freshly prepared 2.5% (vol/vol) glutaraldehyde in CSK for 30 min at room temperature, washed in 0.1 M sodium cacodylate (pH 7.4), and postfixed in 1% osmium tetroxide in the same buffer for 5 min. Cells were dehydrated in a graded series of ethanol. Cells to be embedded in diethylene glycol distearate (DGD; no. 1873; Polysciences) were stained with saturated eosin for localization in the block.

Whole Mounts. For microscopy of whole mounts, the extracted and fixed cells on their nickel grid supports were dehydrated in ethanol and dried through the CO_2 critical point with dehydrated, filtered liquid CO_2 . The dried samples were lightly carbon coated and viewed at 80 kV in the transmission electron microscope.

Resinless Sections. The DGD procedure for resinless sections has been described (10, 11). Cells were grown on Mylar, which is easily peeled off after embedding. Briefly, extracted, fixed cells, dehydrated in ethanol, were transferred in graded steps to butanol and then to molten DGD at 60°C. After 2 hr, samples were cooled to room temperature, the Mylar was removed, and the DGD-embedded cells were sectioned in an ultramicrotome with a glass knife. Sections were picked up on Formvar/carbon-coated copper grids and the DGD was removed with butanol. The sections were transferred to ethanol, critical point dried, and lightly carbon coated.

Scanning Microscopy. Both unextracted and extracted cells on Mylar were fixed, dehydrated, and critical point dried as described above. The Mylar squares were mounted on stubs and sputter coated with gold.

RESULTS

Transmission Electron Microscopy of Saponin-Extracted Whole Mounts. The saponin concentration is a compromise

The publication costs of this article were defrayed in part by page charge payment. This article must therefore be hereby marked "advertisement" in accordance with 18 U.S.C. §1734 solely to indicate this fact.

Abbreviation: DGD, diethylene glycol distearate.
*To whom reprint requests should be addressed.

between an amount of detergent that is sufficient to remove soluble proteins yet low enough to preserve internal mem-

branes. A concentration of 0.01% was arrived at by examining the cell interior in embedment-free whole mounts.

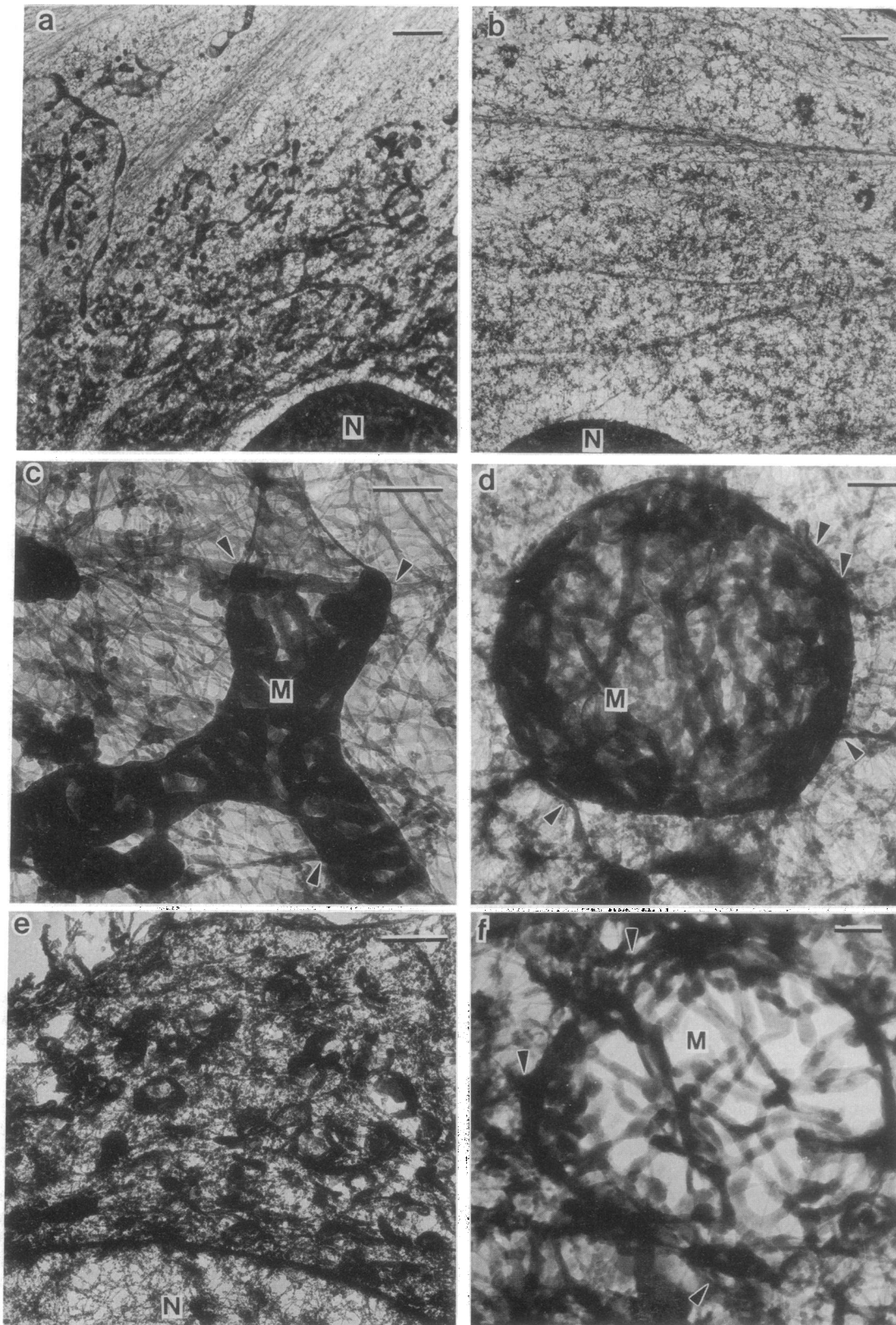


FIG. 1. (a-d) Transmission electron micrographs of extracted cell whole mounts. Cells were grown on nickel grids covered with a carbon-coated Formvar film and extracted. Arrowheads indicate cytoskeleton connections to the membrane. M, mitochondrion; N, nucleus. (a) RASM cells extracted with 0.01% saponin. (Bar = 1 μm .) (b) RASM cells extracted with 0.5% Triton X-100. (Bar = 1 μm .) (c) High magnification of RASM cell mitochondrion suspended in the cytoskeletal network. (Bar = 0.2 μm .) (d) High magnification of HeLa cell mitochondrion suspended in the cytoskeletal network. (Bar = 0.2 μm .) (e) Low magnification of a resinless section of a HeLa cell. (Bar = 1 μm .) (f) High magnification of a resinless section of a HeLa cell showing a mitochondrion in cross-section. (Bar = 0.2 μm .)

Higher saponin concentrations reduced the amount and density of membranes, while lower concentrations left some soluble proteins in the form of characteristic fibrillar material. Otherwise, the extraction conditions were those used previously with Triton X-100.

Fig. 1*a* shows a whole mount of the very flat RASM cell, extracted with saponin. Freed of soluble proteins, the cytoskeleton filaments are clearly visible together with many membrane-bound cytoplasmic organelles enmeshed in the complex networks. The long, sinuous structures have the size and morphology of mitochondria, while the smaller, dense, spherical bodies may be lysosomes, vacuoles, or remnants of endoplasmic reticulum. Fig. 1*b* shows for comparison a RASM cell extracted with Triton X-100, which has a similar cytoskeleton but no cytoplasmic membranes.

Fig. 1*c* shows an elongated RASM cell mitochondrion at higher magnification. The zebra striping is probably cristae, which are rendered electron dense by osmium fixation. There are many cytoskeleton connections to the mitochondrial membrane that are especially notable where the membrane appears to be stretched (arrowheads). Fig. 1*d* shows the very different, nearly spherical mitochondria in a HeLa cell whole mount in which the presumptive cristae lie above one another. There are many apparent connections between the bounding membrane and the cytoskeleton, some of which are indicated (arrowheads).

The depth ambiguities of whole mount images can be resolved in ultrathin resinless sections. Connections between the cytoskeleton and organelle membranes are revealed explicitly without uncertainty as to whether image elements actually join or are in different planes. Fig. 1*e* and *f* show resinless sections of HeLa cells at low and high magnification. The procedure used to produce the resinless sections is compatible with preserving mitochondrial membranes in saponin-extracted cells. The mitochondrion cross-section in Fig. 1*f* shows numerous internal cristae.

Scanning Electron Microscopy of Saponin and Triton X-100-Extracted Cells. Fig. 2 shows the openings in the plasma membrane produced by saponin. The surface of untreated Caski cervical tumor epithelial cells is compared to cells extracted with 0.01% saponin and with 0.5% Triton X-100. The untreated cells were fixed directly, while the remainder were extracted as described in *Materials and Methods*.

Fig. 2*a* shows a typical epithelial cell in tissue culture. Except for microvilli, the plasma membrane is essentially featureless. The high magnification inset shows fine corrugations in the plasma membrane, possibly the result of dehydration or fixation.

Fig. 2*b* shows the plasma membrane after saponin extraction. The overall cell morphology is largely unchanged but the plasma membrane is markedly altered. There are a few large gaps and numerous small openings, which could allow the release of soluble proteins. At high magnification, the plasma membrane has a rough, pebbled appearance, possibly representing remnant lipid-protein domains.

Fig. 2*c* shows the typical morphology of a cell treated with Triton X-100, which extracts most phospholipids. A highly porous lamina, composed of most plasma membrane proteins (17), remains at the cell surface. There are large gaps through which the underlying cytoskeleton can be glimpsed. In contrast to the pebbled appearance after saponin, high magnification shows that the delipidated cell surface now has a much smoother, fine-grained appearance with numerous openings.

Stereoscopic Resinless Section Micrographs of Saponin-Extracted Cells. Stereoscopic micrographs greatly enhance depth perception and show details of cytoskeleton connections to membranes. Fig. 3 shows 0.2- μm sections of saponin-extracted HeLa cells. Mitochondria, with several cristae, appear in cross-section, enmeshed in and connected to numerous cytoskeleton filaments. Stereoscopic viewing shows

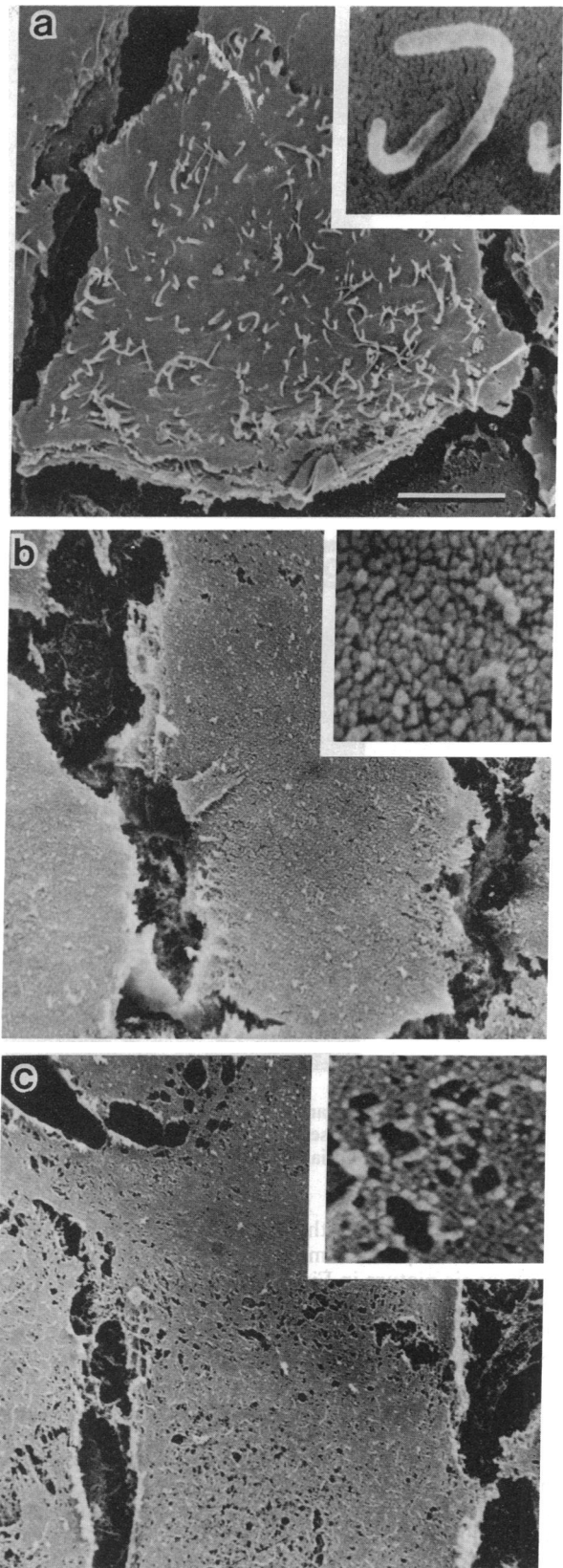


FIG. 2. Scanning micrographs of the apical cell surface at low and high (*Inset*) magnifications. Cells were fixed, dehydrated, critical point dried, and sputter-coated with gold. (a) Unextracted Caski cervical tumor cells. (b) Cells extracted with 0.01% saponin. (c) Cells extracted with 0.5% Triton X-100-extracted cells. (Bar = 5 μm .) (*Insets*, $\times 20,000$.)

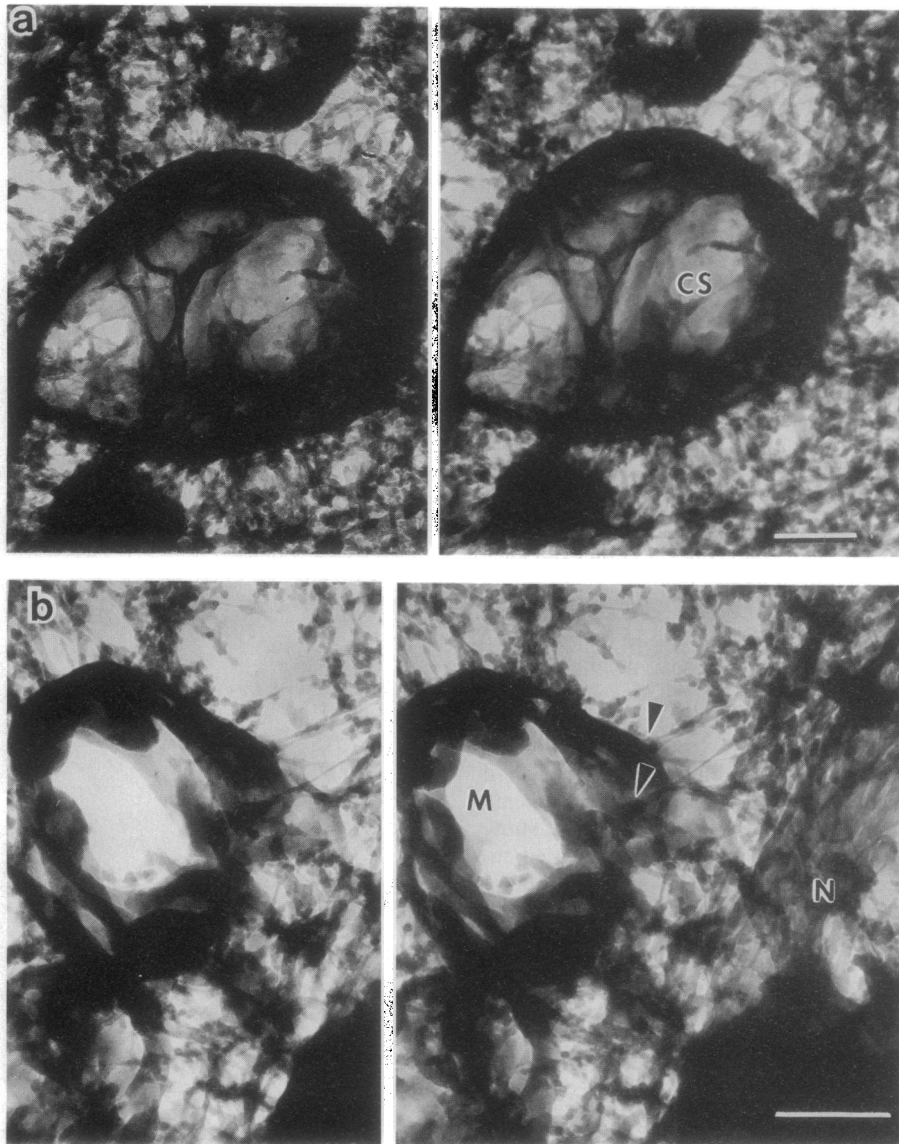


FIG. 3. Stereoscopic transmission micrographs of a resinless section of saponin-extracted HeLa cell. Cells were extracted with 0.01% saponin, fixed, and processed for resinless sections. The tilt angle between the two images was 10° . Arrowheads show cytoskeletal filament connections to mitochondrial membranes. M, mitochondrion; N, nucleus; CS, cytoskeletal fibers. (Bars = $0.2 \mu\text{m}$.)

that the mitochondrion in Fig. 3a is cup shaped and is probably connected to the nexus of cytoskeletal fibers beneath the hemispherical membrane. The higher magnification stereoscopic picture in Fig. 3b shows cytoskeleton filaments clearly terminating at and possibly intertwined with the mitochondrial membrane (arrowheads). These images suggest a role for the cytoskeleton in mitochondrial morphology.

DISCUSSION

Several techniques have been described previously for imaging cellular structures in three dimensions. The rapid-freeze, deep-etch procedure (18) requires special apparatus and produces a platinum replica appreciably thicker than many cytoskeleton elements. The embedment-free whole mounts and resinless sections require no special apparatus, are simple to implement, and afford morphologically accurate depictions of cell structural elements.

Embedment-free electron microscopy, an early electron microscopy technique, was reintroduced by Porter (2-4) using cell whole mounts and a million volt microscope and extended to ultrathin sections made by using polyethylene glycol (19) and later DGD (10, 11) for the removable embed-

ding compound. The techniques were most effective when applied to the cytoskeleton freed of soluble proteins. Here we show that extraction with saponin is an alternative to the usual detergents used to reveal the cytoskeleton and affords embedment-free micrographs of cytoskeleton-membrane interactions.

Saponin, a plant-derived glycoside, reportedly selectively extracts cholesterol (15, 16) from biological membranes, often without destroying their integrity. Whatever its actual mode of action, saponin renders the plasma membrane sufficiently porous (Fig. 2b) to permit soluble proteins to diffuse away. The pebbled appearance of the saponin-treated cell surface may result from remnant phospholipid-protein domains, which are removed by the stronger detergent, Triton X-100 (Fig. 2c). Mitochondrial membranes, having little cholesterol, survive extraction particularly well and are shown here.

Saponin has been used previously in electron microscopy but, with one exception (20), not for embedment-free images of membranes. Saponin has been used combined with fixatives, such as glutaraldehyde, which rapidly cross-link soluble proteins and prevent their extraction (21). Cells have been extracted with saponin alone but viewed by using conven-

tional embedded sections, which cannot show the cytoskeleton (22–24). Embedment-free sections have been made of tissue extracted with saponin but combined with Triton X-100, thus negating the membrane-sparing property of saponin alone (25).

The notable report of Katsumoto and Kurimura (20) recently came to our attention. They used saponin to prepare embedment-free cell whole mounts by a method very similar to ours. The whole mounts were sheared open so as to image, in cross-section, microfilament connections to Con A receptors on the plasma membrane. Their extraction buffer had somewhat lower ionic strength and osmolarity and they usually omitted postfixation with osmic acid, which is necessary to preserve membranes through the temporary embedment in the resinless section procedure.

The initial studies reported here are of mitochondrial membranes and their connections to the cytoskeleton. These membranes largely survive the extraction and temporary embedding steps, although some large gaps are apparent. The pictures show cytoskeleton fibers making extensive connections to mitochondria and sometimes seeming to intertwine with the membrane. These fibers may participate in determining the form of mitochondria and perhaps other organelles.

Compared to the current sophisticated knowledge of the molecules composing cells, we have but elementary awareness of their assembly into cell architecture. This is due, in part, to the inappropriateness of conventional electron microscopy to the study of cell structure. The procedure described here extends the powerful techniques of embedment-free microscopy to the organization of membranes.

1. Pease, D. C. & Porter, K. R. (1981) *J. Cell Biol.* **91**, 287–292.
2. Porter, K. R. (1984) *J. Cell Biol.* **99**, 3s–12s.
3. Porter, K. R. & Stearns, M. E. (1981) *Methods Cell Biol.* **22**, 53–75.
4. Porter, K. R. & Wolosewick, J. J. (1977) *J. Electron Microsc. Suppl.* **26**, 15–20.
5. Lenk, R., Ransom, L., Kaufmann, Y. & Penman, S. (1977) *Cell* **10**, 67–78.
6. Lenk, R. & Penman, S. (1979) *Cell* **16**, 289–301.
7. Penman, S., Capco, D. G., Fey, E. G., Chatterjee, P., Reiter, T., Ermish, S. & Wan, K. M. (1983) *Mod. Cell. Biol.* **2**, 385–415.
8. Schliwa, M. & van Blerkom, J. (1981) *J. Cell Biol.* **90**, 222–235.
9. Schliwa, M. (1982) *J. Cell Biol.* **92**, 79–91.
10. Fey, E. G., Krockmalnic, G. & Penman, S. (1986) *J. Cell Biol.* **102**, 1653–1665.
11. Capco, D. G., Krockmalnic, G. & Penman, S. (1984) *J. Cell Biol.* **98**, 1878–1885.
12. Jackson, D. A. & Cook, P. R. (1988) *EMBO J.* **7**, 3667–3678.
13. Nickerson, J. A., He, D. C. & Penman, S. (1990) in *The Eukaryotic Nucleus: Molecular Biochemistry and Macromolecular Assemblies*, eds. Strauss, P. R. & Wilson, S. H. (Telford, London).
14. He, D. C., Nickerson, J. A. & Penman, S. (1990) *J. Cell Biol.* **110**, 569–580.
15. Bangham, A. D. & Horne, R. W. (1962) *Nature (London)* **196**, 952–953.
16. Glauert, A. M., Dingle, J. T. & Lucy, J. A. (1962) *Nature (London)* **196**, 953–955.
17. Ben-Ze'ev, A., Duerr, A., Solomon, F. & Penman, S. (1979) *Cell* **17**, 859–865.
18. Heuser, J. E. & Kirchner, M. W. (1980) *J. Cell Biol.* **86**, 212–234.
19. Wolosewick, J. (1980) *J. Cell Biol.* **86**, 675–681.
20. Katsumoto, T. & Kurimura, T. (1988) *Biol. Cell.* **62**, 1–10.
21. Maupin, P. & Pollard, T. D. (1983) *J. Cell Biol.* **96**, 51–62.
22. Gotoh, H., Takenaka, T. & Shozushima, M. (1983) *Cell Struct. Funct.* **8**, 11–18.
23. St. John, P. A., Froehner, S. C., Goodenough, D. A. & Cohen, J. B. (1982) *J. Cell Biol.* **92**, 333–342.
24. Willingham, M. C., Yamada, S. S. & Pastan, I. (1978) *Proc. Natl. Acad. Sci. USA* **75**, 4359–4363.
25. Ishii, M., Miyazaki, Y., Otsuki, M., Suzuki, H. & Goto, Y. (1985) *Tohoku J. Exp. Med.* **147**, 317–329.